Anal. Chem. **2007,** *79,* 7740−7747

Stochastic Single-Molecule Videomicroscopy Methods To Measure Electrophoretic DNA Migration Modalities in Polymer Solutions above and below Entanglement

Thomas N. Chiesl,[†] Ryan E. Forster,[‡] Brian E. Root,[‡] Michael Larkin,[†] and Annelise E. Barron*[,†,§]

Department of Chemical and Biological Engineering, Department of Chemistry, and Department of Materials Science and Engineering, Northwestern University, Evanston, Illinois 60208

We have studied the effects of polymer molar mass and concentration on the electrophoretic migration modalities of individual molecules of DNA in LPA, HEC, and PEO solutions via epifluorescent videomicroscopy. While both transient entanglement coupling (TEC) and reptation have been studied in the past, the transition between them has not. Understanding this transition will allow for polymer network properties to be optimized to enhance the speed and resolution of DNA separations in microfluidic devices. Near the overlap threshold concentration, C^*, TEC is the dominant observed mode of DNA migration, and the observation frequency of TEC increases with increasing polymer molar mass. As polymer concentration is increased, observed TEC events reduce to zero while DNA reptation events become the only detected mechanism. Individual DNA molecules undergoing both migration mechanisms were counted in solutions of varying polymer molar masses and concentrations and were plotted against a dimensionless polymer concentration, C/C^*. The data for LPA reduce to form universal curves with a sharp increase in DNA reptation at $\sim 6.5C^*$. Analogous transition concentrations for PEO and HEC were observed at $5C^*$ and $3.5C^*$, respectively, reflecting the different physical properties of these polymers. This transition correlates closely with the polymer network entanglement concentration, C_e, as measured by rheological techniques. The electrophoretic mobility of λ-DNA in LPA polymer solutions was also measured and shows how a balance can be struck between DNA resolution and separation speed by choosing the desired prevalence of DNA reptation.

Polymer solutions have long been studied for their interesting nonlinear viscoelastic response properties. Pioneering work in the field by de Gennes discussed the reptation of polymer molecules,[1] the dynamics of confined polymer chains,[2] and the dynamics of entangled polymer solutions.[3,4] Graessley further expanded upon this work and defined regions of semidilute and concentrated unentangled and entangled polymer solutions.[5−7] Important to the rheological discussion of polymer solution viscosities are two critical parameters: C^*, the polymer overlap concentration,[8,9] and C_e,[10,11] the polymer entanglement concentration, which define the dilute, semidilute, and entangled regions. In the past decade, aqueous polymer solutions in the entangled and semidilute concentration regimes have become important in the field of electrophoretic DNA separations as applied to forensic genotyping[12,13] and DNA sequencing.[14,15] Theoretical predictions along with some experimental evidence have postulated and described three basic electrophoretic DNA separation modalities: transient entanglement coupling,[16−20] Ogston-type sieving,[21] and reptation.[22−24] In this work, we have utilized single-molecule epifluorescence

* Corresponding author. Present address: Department of Bioengineering, 318 Campus Drive, James H. Clark Center, Room W300B, Stanford University, Stanford, CA 94305. Tel: (650) 721-1151. Fax: (650) 723-8544. E-mail: aebarron@stanford.edu.

[†] Department of Chemical and Biological Engineering.

[‡] Department of Materials Science and Engineering.

[§] Department of Chemistry (by courtesy).

(1) Gennes, P. G. D. *J. Chem. Phys.* **1971**, *55*, 572−579.
(2) Brochard, F.; Gennes, P. G. D. *J. Chem. Phys.* **1977**, *67*, 52−56.
(3) Gennes, P. G. D. *Macromolecules* **1976**, *9*, 594−598.
(4) Gennes, P. G. D. *Macromolecules* **1976**, *9*, 587−593.
(5) Graessley, W. W. *Adv. Polym. Sci.* **1974**, *16*, 164−179.
(6) Graessley, W. W. *Polymer* **1980**, *21*, 258−262.
(7) Graessley, W. W. *Adv. Polym. Sci.* **1982**, *47*, 67.
(8) Daoud, M.; Cotton, J. P.; Farnoux, B.; Jannink, G.; Sarma, G.; Benoit, H.; Duplessix, R.; Picot, C.; Gennes, P. G. d. *Macromolecules* **1975**, *8*, 804−818.
(9) Ying, Q.; Chu, B. *Macromolecules* **1987**, *20*, 362−366.
(10) Heo, Y.; Larson, R. *J. Rheol.* **2005**, *49*, 1117−1128.
(11) Jimenez-Regalado, E.; Selb, J.; Candau, F. *Macromolecules* **2000**, *33*, 8720−8730.
(12) Butler, J. M.; Buel, E.; Crivellente, F.; McCord, B. R. *Electrophoresis* **2004**, *25*, 1397−1412.
(13) Goedecke, N.; McKenna, B.; El-Difrawy, S.; Carey, L.; Matsudaira, P.; Ehrlich, D. *Electrophoresis* **2004**, *25*, 1678−1686.
(14) Zhou, H.; Miller, A.; Sosic, Z.; Buchholz, B.; Barron, A.; Kotler, L.; Karger, B. *Anal. Chem.* **2000**, *72*, 1045−1052.
(15) Paegel, B.; Emrich, C.; Weyemayer, G.; Scherer, J.; Mahies, R. *Proc. Natl. Acad. Sci. U.S.A.* **2002**, *99*, 574−579.
(16) Barron, A. E.; Soane, D. S. S.; Blanch, H. W. *J. Chromatogr., A* **1993**, *652*, 3−16.
(17) Barron, A.; Blanch, H.; Soane, D. *Electrophoresis* **1994**, *15*, 597−615.
(18) Shi, X.; Hammond, R.; Morris, M. *Anal. Chem.* **1995**, *67*, 1132−1138.
(19) Barron, A. E.; W. M., S.; Blanch, H. W. *Electrophoresis* **1996**, *17*, 744−757.
(20) Sunada, W.; Blanch, H. *Biotechnol. Prog.* **1998**, *14*, 766−772.
(21) Slater, G.; Kenward, M.; McCormick, L.; Gauthier, M. *Curr. Opin. Biotechnol.* **2003**, *14*, 58−64.
(22) Kantor, R.; Guo, X.; Huff, E.; Schwartz, D. *Biochem. Biophys. Res. Commun.* **1999**, *258*, 102−108.
(23) Sartori, A.; Barbier, V.; Viovy, J. *Electrophoresis* **2003**, *24*, 421−440.

10.1021/ac071160x CCC: $37.00
Published on Web 09/18/2007

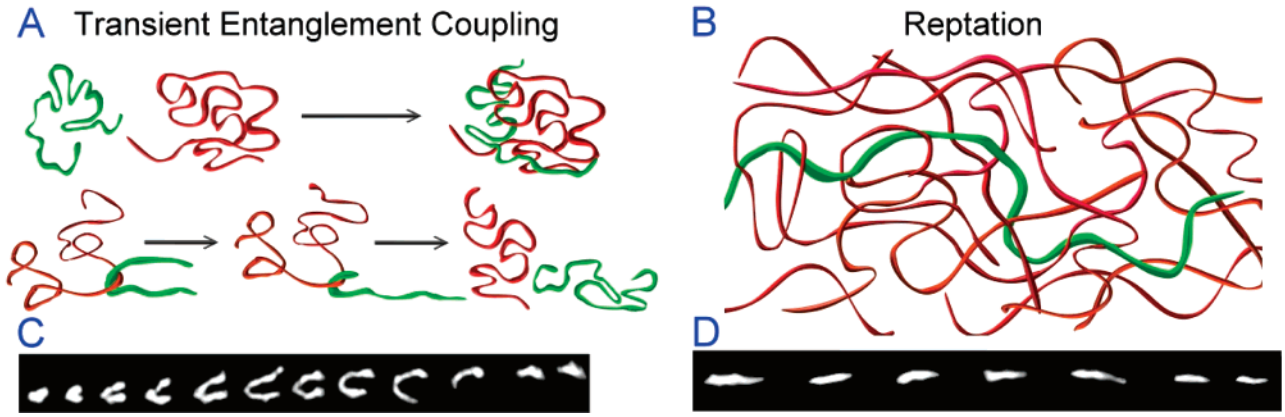

Figure 1. Schematic representations of polymer conformations (red) presented with a DNA molecule (green) undergoing a given migration modality. In dilute solutions (A), the polymer chain is relatively isolated and in a globular state. The polymer does not have entanglements with other polymers to create a robust network, and as a result, DNA interacts with polymer via a transient entanglement coupling mechanism. As polymer concentration is increased (B), polymer chains develop multiple entanglements and create a network in which DNA must snake its way through the matrix via reptation. Representative still-frame captures of λ-DNA undergoing the two predominant electrophoretic migration mechanisms, (C) transient entanglement coupling and (D) reptation, are included. Both images captured in a 2% w/w polyacrylamide solution with a molecular mass of 1.2 million g/mol at 100 V/cm.

videomicroscopy to directly observe DNA molecules undergoing both transient entanglement coupling and reptation mechanisms in linear polymer solutions and have related the mechanistic transition to universal polymer solution physical characteristics. The mode of DNA migration largely impacts the obtainable speed and resolution in electrophoretic separations, and therefore, this information should enable the optimization of separation matrixes for microchannel electrophoresis systems.

Each of these electrophoretic separation mechanisms and polymer solution environments are further discussed below; however, for clarity, we present schematics and single-molecule videomicroscopic images of each electrophoretic DNA separation mechanism in Figure 1. Polymer molecules have been represented in red and DNA molecules in green. Figure 1A illustrates, in a series of steps, the transient entanglement coupling mechanism as often seen in dilute polymer solutions, and Figure 1B shows a schematic of DNA reptation through an entangled linear polymer solution. A series of image captures of a fluorescently labeled DNA molecule (λ-DNA, 48.5 kbp) undergoing transient entanglement coupling is shown in Figure 1C, and a DNA molecule in reptation is shown in Figure 1D. Representative videos of DNA undergoing each migration mode can be found in the Supporting Information

Dilute Polymer Solutions. Transient Entanglement Coupling. In dilute polymer solutions, polymer molecules behave as flexible, isolated chains where the average distance between chains is larger than the chain size. As the polymer concentration is increased to C^*, the average polymer concentration in the solution becomes equivalent to the average concentration of polymer within a single polymer coil. Classically, this has been represented schematically by a series of spheres just beginning to touch each other with the radius of these spheres being equivalent to the radius of gyration of the solvated polymer chain. It is important to note that at this concentration the polymer chains are just beginning to share probable occupied volume within their random walks. While segments of other polymer coils may intrude upon these shared volumes, polymer−polymer interactions are weak and a low likelihood exists that many long-lasting interpolymer entanglements are stable. Thus, the polymer organization is relatively "loose" and susceptible to deformation with moderate amounts of local force. Barron et al. first demonstrated the size-based separation of DNA in dilute and ultradilute polymer solutions and hypothesized this to occur via a transient entanglement coupling mechanism (TEC).[16,17] This migration modality was later confirmed by direct observation using epifluorescence videomicroscopy.[18,20,24,25] Figure 1C presents a series of captured images showing a DNA molecule undergoing a representative transient entanglement coupling event in a polyacrylamide solution. In TEC, DNA molecules collide with individual polymer chains in solution or have multiple collisions with successive polymer chains. The DNA and polymer molecules entangle with each other, and the polymer molecules effectively cause the DNA molecule to open from its globular shape into a "U" configuration. The DNA drags the polymer chain or chains until the polymer slides off the DNA (or vice versa) and disentanglement occurs.[21,26] Size-based separation of DNA occurs due to differing frequencies of DNA−polymer collisions and differing rates of DNA−polymer disentanglement.[16,17,26] After disentanglement, the DNA chain contracts back into a globular conformation.

Entangled Polymer Solutions. DNA Reptation. In polymer solutions with concentrations considerably above C^*, polymers no longer exist as isolated chains and have many physical constraints or entanglements involving neighboring chains. Highly entangled linear polymer solutions have taken the place of chemically cross-linked gels for most analytical DNA separations due to their ability to flow and be loaded into capillaries as well as to provide high-performance separations. Unlike chemically cross-linked polymer solutions, the lifetimes of entanglements found in linear polymer solutions are short and change with various polymer solution properties.[27] Generally, increasing the

(24) Chiesl, T. N.; Putz, K. W.; Babu, M.; Mathias, P.; Shaikh, K. A.; Goluch, E. D.; Liu, C.; Barron, A. E. *Anal. Chem.* **2006**, *78*, 4409−4415.
(25) Starkweather, M.; Muthukumar, M.; Hoagland, D. *Macromolecules* **2000**, *33*, 1245−1253.
(26) Hubert, S.; Slater, G.; Viovy, J. *Macromolecules* **1996**, *3*, 1006−1009.

concentration of polymer increases the entanglement lifetime, which relates to the relaxation time of the network. At a given polymer concentration, larger molar mass polymers will form more entanglements per chain than smaller molar mass polymers and thus exhibit a higher solution viscosity and greater network robustness. However, the average mesh size of these networks is independent of the degree of polymerization (polymer molar mass) and is only a function of polymer concentration.[27] These properties of polymer solutions have long been established via standard polymer rheology techniques.

When DNA is electrophoresed through entangled linear polymer solutions, it can migrate via one of two mechanisms, Ogston-type sieving or reptation. For Ogston-type sieving, the assumption is made that the polymer network is a rigid structure. Coiled DNA migrates undeformed through fixed pores at a rate proportional to the fraction of the pores that is equal to or larger in size than the size of the DNA.[28] Ogston-type sieving is typically seen only for smaller DNA fragments in most electrophoresis sieving materials and may not occur in non-cross-linked linear polymer solutions for larger sized DNA. The DNA reptation model arises from situations in which DNA must migrate though a polymer network with pore sizes that are smaller than the globular DNA molecule. In order to migrate in an electric field, the DNA molecule must elongate and wind in a snakelike fashion though the obstacle course the polymer network presents. A representative example of DNA reptation can be seen in Figure 1D, where a series of images shows the undulating behavior of a stretched DNA molecule. Under low fields, the mobility of DNA fragments in these polymer networks is inversely proportional to DNA size. Additionally, higher electric field strengths tend to orient the DNA molecule more strongly in the direction of the electric field and size-based separation of DNA is diminished.[29−32]

Semidilute Polymer Solutions. In the semidilute concentration regime, polymer molecules will be neither fully isolated nor fully entangled but would exist in states where few entanglement points exist and the lifetimes of these entanglements are brief.[27] The polymer network in this regime is more resilient to deformation than in dilute polymer solutions, but not robust enough to withstand minor disruptions caused by DNA migration. Within this concentration regime, it is expected that the transition in the DNA separation mechanism from transient entanglement coupling to reptation should occur, and for potential hybrid migration modalities to be present. Here, we have investigated the transition between electrophoretic DNA migration mechanisms and correlated it to two polymer concentrations, C^* and C_e. C^* represents the overlap threshold concentration. C_e is a true polymer entanglement concentration where the network becomes robust and elastically effective.[6,11,27]

MATERIALS AND METHODS

Polymer Synthesis and Characterization. All DNA electrophoresis experiments were conducted in 0.5× TTE buffer (49 mM Tris, 49 mM TAPS, 2 mM EDTA, pH 8.4, all from Amresco, Inc., Solon, OH). Hydroxyethylcellulose (HEC) was obtained from Aldrich (St. Louis, MO) and Aqualon Hercules, Inc. (Natrosol Brand, Wilmington, DE), and poly(ethylene oxide) (PEO) was obtained from Aldrich (St. Louis, MO) and Acros Organics (Geel, Belgium) and used without further purification. Linear polyacrylamide (LPA) was synthesized using standard free-radical solution polymerization techniques.[33] Briefly, acrylamide monomer (Amresco, Inc., Solon, OH) was dissolved in 300 mL of water at 3% w/w inside a 500-mL four-neck reaction flask (Kontes, Vineland, NJ). The solution was stirred and bubbled with nitrogen for 30 min to remove oxygen, and 0.02 g of 4,4′-azobis(4-cyanovaleric acid) initiator was added. The solution was then placed in a 50 °C water bath and allowed to react for 4 h. Polymer was purified by first cooling the solution to room temperature and then placing it into Spectra/Por cellulose ester dialysis membranes with 100 000 g/mol molecular weight cutoff (Spectrum, Gardena, CA). Dialysis water was frequently changed over two weeks, and polymers were recovered by freeze-drying. Three linear polyacrylamides with different molecular weights were synthesized and used for this study.

Polymer molar mass was characterized via tandem gel permeation chromatography-multiangle laser light scattering (GPC-MALLS) using a Waters 2690 Alliance Separations Module (Milford, MA) as previously described by Buchholz et al.[14] Polymer samples are first fractionated by GPC using OHpak columns SB-806 HQ, SB-804 HQ, and SB-802.5 HQ (Shodex, New York) connected in series with an on-line multiple-angle laser light-scattering system with a DAWN DSP laser photometer (Wyatt Technology, Santa Barbara, CA) and refractive index measurements made by an Optilab DSP interferometric refractometer (Wyatt Technology). The flow rate was 0.3 mL/min, and the mobile phase consisted of 100 mM NaCl, 50 mM NaH_2PO_4, and 200 ppm NaN_3. The GPC-MALLS data were processed using WTC ASTRA 4.73 software from Wyatt Technology. Weight-average molar mass (M_w), polydispersity index (PDI), and *z*-average radius of gyration (R_z) were calculated using the Berry method with a known AUX constant and assumption of 100% polymer recovery.[14] All analyses were repeated at least three times. A summary of polymer characteristics, for polymers used in this study, can be found in Table 1.

Viscosity Measurements. Rheological testing of polymer solutions was performed with a Paar Physica (Glen Allen, VA) modular compact rheometer, MCR 300, using the DG26.7 fixture. The DG26.7 is a double-gap cylinder measuring system with large surface area, recommended by Paar Physica for measuring low solution viscosities. The temperature was maintained at 25 °C by using a Peltier system, model TEZ 150P-C, connected to an external water bath. Several polymer solutions with concentrations ranging from 0.02 to 4% w/w were prepared, and for each test, 3.6 mL of solution was pipetted into the annulus of the fixture. A shear rate sweep test was conducted, which consists of at least a 45-s pause before the experiment to ensure the sample has come to a near-equilibrium state. The shear rate sweep ranged from 10 to 1000 s^{-1} using a logarithmic ramp and collected 21 data points during each sweep. A "blank" sample (without polymer) of aqueous 0.5× TTE buffer was analyzed under the same conditions

(27) Rubinstein, M.; Colby, R. H. *Polymer Physics*, 2 ed.; Oxford University Press: New York, 2003.
(28) Rodbard, D.; Chrambach, A. *Proc. Natl. Acad. Sci. U.S.A.* **1970**, *65*, 970−977.
(29) Southern, E. *Anal. Biochem.* **1979**, *100*, 319−323.
(30) Lerman, L.; Frisch, H. *Biopolymers* **1982**, *21*, 995−997.
(31) Stellwagen, N. *Biopolymers* **1985**, *24*, 2243−2255.
(32) Ueda, M.; Oana, H.; Baba, Y.; Doi, M.; Yoshikawa, K. *Biophys. Chem.* **1998**, *71*, 113−123.
(33) Chiesl, T.; Shi, W.; Barron, A. *Anal. Chem.* **2005**, *77*, 772−779.

Table 1. Summary of Polymer Properties Used in This Study[a]

	M_W ($\times 10^{-6}$ g/mol)	R_Z (nm)	PDI	C^* (% w/w)
LPA−1	0.6	64	1.81	0.28
LPA−2	1.2	74	2.18	0.15
LPA−3	3.5	98	1.88	0.08
HEC−1	0.36	69	3.15	0.45
HEC−2	2.66	196	1.57	0.10
PEO−1	0.33	66	3.32	0.75
PEO−2	1.20	80	1.89	0.30
PEO−3	3.48	115	1.72	0.18

[a] Polymer molar masses ranged from 350 000 to 4 million g/mol. Weight-average polymer molar mass, *z*-average radius of gyration, and polydispersity index were determined via tandem GPC-MALLS.[14] C^* was measured experimentally via rheological measurements.

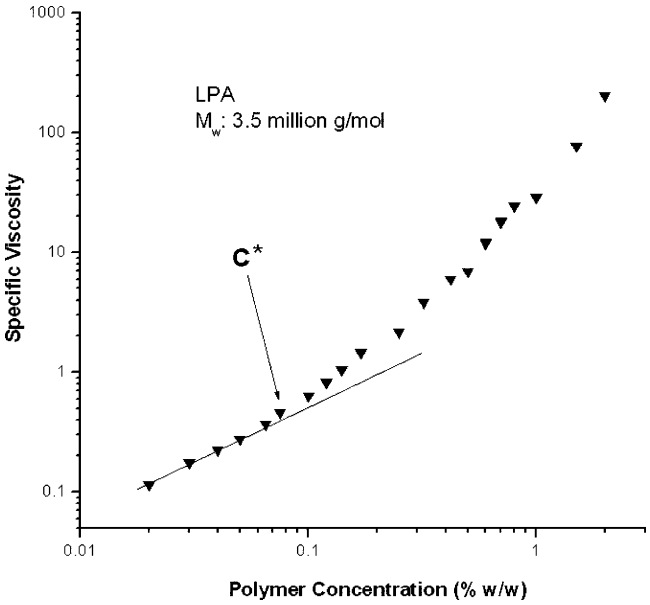

Figure 2. Specific viscosity vs polymer concentration for LPA with a molecular mass of 3.5 million g/mol. C^* is calculated as the first point to significantly deviate from linearity. In this case, C^* is 0.08% w/w as indicated by the arrow.

to obtain a value for pure solvent viscosity (1.13 cP). The zero-shear specific viscosity was plotted as a function of polymer concentration (% w/w) on a log−log scale, and a line was fit to data points in the lower concentration range. C^* was identified as the first point to deviate significantly from linearity.[16] Several viscosity measurements at polymer concentrations above and below C^* were taken in order to ensure accurate determination of the overlap concentration. A representative plot generated via this method can be seen in Figure 2, where C^* has been determined to be 0.08% w/w for this linear polyacrylamide with a molecular mass of 3.5 million g/mol. C^* values for the polymers analyzed for this study are included in Table 1.

Single-Molecule Visualization and Sample Preparation. Visualization of electrophoresing DNA molecules was accomplished using an epifluorescence videomicroscopy system as previously described.[24] Briefly, our laboratory-built setup consists of a 100-W mercury lamp light source directed into a Nikon TE2000 U inverted epifluorescence microscope with a FITC filter cube (Chroma Technology, Brattleboro, VT). The light is focused through a Nikon CFI 100× NA 1.4, 0.133-mm working distance apochromatic oil immersion microscope objective, collected through the same objective and directed into a VS4-1845 Generation 3 image intensifier (Videoscope International, Dulles, VA) where it is focused onto a 0.5-in. CCD, TM-6710-CL camera (JAI Pulnix, Sunnyvale, CA). This high-speed camera has an adjustable frame rate up to 120 frames/s with full resolution of 648 × 484 pixels. Videos and images are captured onto a computer (Dell, 3 GHz processor, one gigabyte of memory) via camera link technology to a PIXCI control board (Epix Inc., Buffalo Grove, IL), and the capture is controlled through XCAP-STD (Epix Inc.) software. Videos were adjusted for brightness and contrast using Adobe Premier 6.5 software, and individual frames were exported to Adobe Photoshop 7.0 for background subtraction and image smoothing.

Linearized λ-phage DNA (48.5 kbp, N3011S, New England Biolabs, Ipswich, MA) was fluorescently stained with YOYO-1 (Molecular Probes/Invitrogen, San Diego, CA) and mixed into each respective polymer solution.[34] Catalase, glucose, glucose oxidase (Fisher Scientific, Pittsburgh, PA), and β-mercaptoethanol (Sigma-Aldrich, St. Louis, MO) were added into the solution to reduce the amount of detrimental oxygen and free-radical interactions with DNA when exposed to air and light.[35] Pipet tips were cut wider with a razor blade to avoid shearing and breaking the DNA. Microchannels used for DNA imaging are composed of a Sylgard 184 poly(dimethylsiloxane) (PDMS; Fisher Scientific) top piece and a glass coverslip of thickness number 1.5 (Fisher Scientific). The PDMS cover is formed by degassing a 10:1 ratio (by weight) prepolymer to curing agent mixture solution and then pouring this mixture on top of thinly cut (1−2 mm) slices of Scotch Magic Tape (50−60-μm thickness). The PDMS top piece was cured in a vacuum chamber overnight, cut to fit on a cover slip, peeled off, and placed on the glass coverslips. The stained DNA/polymer solution was pipetted onto one end of the microchip and allowed to wick into the microchannel by capillary action. Another equal-volume drop of solution was placed at the other end to serve as a buffer reservoir. The solution was allowed to equilibrate for 1 min to dissipate any latent hydrodynamic or capillary-based flows. The electric field was applied via platinum-tipped electrodes powered by a home-built circuit containing a number of 9-V batteries connected in series to give the desired electric field and polarity.

Counting Method for Imaged ds-λ DNA. At least two 30-s videos were recorded of the λ-DNA migrating through polymer solutions at each concentration, and on average, 30−40 DNA molecules undergoing a given range of separation modalities were recorded and analyzed. At least 10 concentrations of each molar mass and each polymer were examined and ranged from 0.01 to 4% w/w. Experiments were conducted at field strengths of ~100 V/cm, as this field strength yielded a compromise between easy-to-observe (and experimentally relevant) DNA migration speed and relative ease of data analysis. These field strengths also begin to approach field strengths commonly used for DNA capillary electrophoresis experiments, which are typically 150−200 V/cm. The videos were analyzed frame-by-frame to determine which

(34) Randal, G. C.; Doyle, P. *Macromolecules* **2005**, *38*, 2410−2418.
(35) Yanagida, M.; Morikawa, K.; Hiraoka, Y.; Matsumoto, S.; Uemura, T.; Okada, S. *Applications of Fluorescence in the Biomedical Sciences*; Alan R. Liss, Inc.: New York, 1986.

migration mechanisms were taking place. After the videos for each concentration had been collected, the information regarding the polymer type and concentration for the 600 000 g/mol LPA data was then made "blind" to two observers, who counted the occurrences of each mechanism. All of the other videos collected were counted with known concentrations; however, random videos were selected from each polymer group to check for biases. Comparison of the tally achieved for both observers did not show a significant difference greater than 10%. The DNA were categorized into three possible groups related to DNA conformation during electrophoresis through polymer solutions, globular (no observed mechanism), TEC, and reptation. For a DNA molecule to be considered, it was necessary that it traverse a minimum of half of the plane of view while remaining in focus. A DNA molecule that remained in a "round" conformation and was not observed to undergo any visible deformation or separation mechanism was counted as a globular DNA. A TEC event was identified by the DNA starting in the compact spherical form and subsequently taking a U-shape, which required that the two ends of the molecule extend out equidistant or near-equidistant in the direction of the applied electric field. A reptation event was recorded when an elongated DNA remained stretched for a minimum of five consecutive frames (but this often occurred for much longer) with undulating motion. Each occurrence of transient entanglement coupling and reptation observed in the videos was recorded and tallied with respect to the corresponding polymer concentration.

Mobility Measurements. The electrophoretic mobility of λ-DNA was measured using a MegaBACE 1000 (Amersham Biosciences, Piscataway, NJ) 96-capillary array electrophoresis instrument with 75-μm-i.d., 40-cm detection length, capillaries precoated with covalently bonded LPA. λ-DNA was first labeled with YOYO-1 (without additional proteins and antioxidants) and then diluted by the addition of 300 μL of deionized water. The solution was loaded into a 96-well plate for injection via application of a 47 V/cm field for 30 s. The data for each run were then exported into a text file, and migration times were converted into mobilities and tabulated.

RESULTS AND DISCUSSION

DNA molecules were imaged in solutions of water-soluble polymers having three different chemical structures: HEC, PEO, and LPA. These three polymers were specifically chosen because they have all been used extensively for separating DNA via capillary electrophoresis.[22,36] Polyacrylamide and PEO, each of three different molar masses, and HEC with two different molar masses were examined (Table 1). These polymer molar masses ranged from 330 000 to 3 500 000 g/mol and were chosen because they span those traditionally used in capillary or microchip electrophoresis of DNA. Additionally, these three polymers have different inherent chain flexibilities, from the very flexible PEO to the relatively stiff cellulose. The largest molar mass polyacrylamide had ~48 000 monomer units (weight average) and the smallest LPA had 8200 monomer units. The largest molar mass PEO had 80 000 monomer units, and the smallest PEO has 7500. As a comparison, the fluorescently labeled DNA comprises 48 000 base pairs. C^*, the overlap threshold concentration, for each of these polymers was determined experimentally by rheology,[16,19] in the manner shown in Figure 2, and decreased with increasing polymer molar mass as expected (Table 1). In general, at similar molar masses, C^* values for polyacrylamide are less than those of PEO and slightly greater than those of HEC. A complete summary of polymer properties examined in this work including overlap threshold data can be found in Table 1.

Videos of DNA migrating in each polymer solution were acquired over a range of polymer concentrations, and the number of globular, TEC, and reptating DNA migration modalities were recorded. As a general observation, TEC was the dominant mode of migration for DNA in polymer solutions at low concentrations (concentrations below or near C^*), while at higher concentrations, reptation became the dominant mechanism. Due to the large size of the λ-DNA (48 000 base pairs) and the relatively high electric field strength used for these single-molecule imaging experiments, we did not observe pure Ogston-type sieving behavior in these visualization experiments. On occasions in which we did lower the field strength to ~10−20 V/cm, the directional behavior of DNA migration became more random and less biased, or oriented, with the direction of the electric field. However, at these lower field strengths, photobleaching became problematic and not as many DNA molecules could be accurately observed per experiment. No noticeable trend in the type or amount of a given mechanism was discovered to correlate with variations in the concentration of observed DNA present in these polymer solutions; however, background fluorescence was significantly reduced when smaller amounts of DNA were used.

DNA molecules were electrophoresed through polymer solutions of several different concentrations, for each molar mass, and the number of DNA molecules observed to undergo each type of migration modality was tabulated. At low polymer concentrations, DNA remaining in the globular state or out-of-focus DNA accounted for the majority of events, followed by transient entanglement coupling with a few isolated and brief reptation events. The number of TEC events was relatively constant with polymer concentration for each LPA polymer molar mass until an abrupt decrease near 1% w/w LPA. It is near this concentration that the reptation mechanism becomes prevalent. In conditions where TEC was the dominant migration modality, at lower polymer solution concentrations near C^*, the absolute amount of DNA observed undergoing the transient entanglement coupling mechanism increased as a function of increasing polymer molar mass. Figure 3 shows the percentage of DNA molecules observed undergoing the transient entanglement coupling mechanism as a function of polymer concentration for LPA polymers with three different average molar masses. For the 600 000, 1.2 million, and 3.5 million g/mol LPA polymers, the absolute percentage of TEC migration was found to be 15−20, 35−43, and 45−51%, respectively. This is in fairly good agreement with the observations of Barron et al.[16,17,19] and with the theory of Hubert et al.[37] who have postulated that the mean entanglement time is effectively a function of polymer length given a constant size of DNA. Thus, two factors contribute to our higher observation rate of TEC for larger molar mass polymers, a longer mean collision time and a higher size-based probability of collision.

(36) Albargheuthi, M. N.; Barron, A. E. *Electrophoresis* **2000**, *21*, 4096−4111.

(37) Hubert, S. J.; Slater, G. W.; Viovy, J.-L. *Macromolecules* **1996**, *29*, 1006−1009.

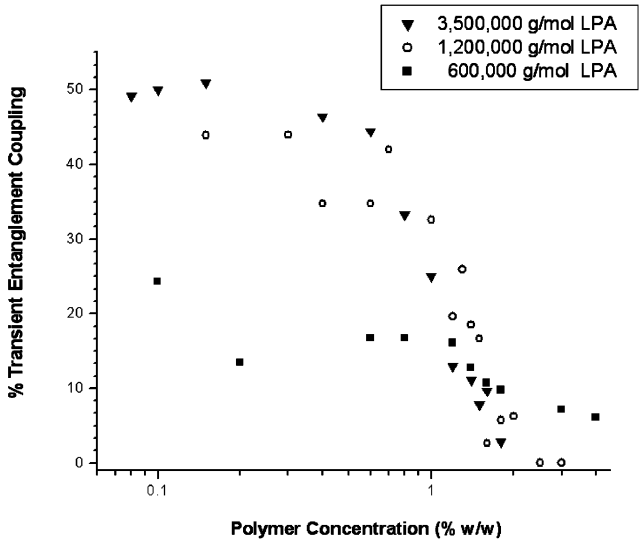

Figure 3. Transient entanglement coupling events observed vs polymer concentration for three LPA polymers. The highest percentage of TEC observed occurs with the largest molar mass polymer.

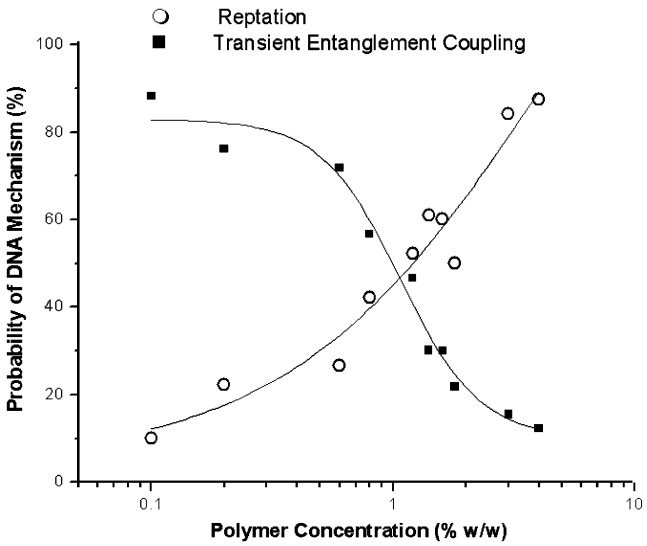

Figure 4. Probability of DNA molecules visualized with a particular mechanism is plotted as a function of concentration for a polymer of molar mass 600 000 g/mol. Approximately 40 molecules at each concentration were counted during a 30-s (1200 frames) video capture. The concentration was unknown to the counter. The crossover transition from transient entanglement coupling to full reptation occurs near 1.5% w/w for this polymer.

In many LPA polymer solutions, at concentrations near 1% w/w, significant occurrences of both transient entanglement coupling and DNA reptation were observed. For higher concentrations in which reptation is dominant, we observed that nearly all DNA molecules are undergoing reptation with a rare TEC event. We have made the assumption that, at lower concentrations, where TEC is the dominant mechanism, the DNA observed to follow no predominant mechanism (globular DNA) has not had adequate observation time within our field of view to form the intermediate "U-shaped" TEC event to occur. Because the start and finish of transient entanglement coupling events appear essentially identical to globular DNA, as shown in Figure 1C, we have made the conclusion that if our spatial field of view had been larger or if we were to track these globular DNAs as they progressed downstream, that most likely they would undergo an event with equal probability as the events observed. Henceforth, we have plotted the probability of each mechanism as the ratio of the percentage of the total nonglobular events counted. As a result of this assumption, the probability of a TEC event is simply 100% minus the probability of reptation. The percentage of each mechanism was plotted against the respective polymer concentrations to determine which migration mechanism was dominant, as a function of increasing polymer concentration. An example plot is given in Figure 4 for DNA molecules observed migrating in polyacrylamide solutions with molecular masses of 600 000 g/mol. In the relatively low polymer concentration range from 0.1 to 0.8% w/w, transient entanglement coupling is observed to be the dominant separation mechanism. The 50% crossover point between mechanisms occurs at a concentration of ~1.6% w/w and full DNA reptation is realized at ~3−4% w/w polymer. In correlation with polymer solution dynamics, the 50% mechanism crossover point for this LPA occurs at a concentration significantly greater than C^*, which was experimentally found to be 0.28% w/w. A sigmoidal curve, often used to model dosage response, was used to fit the data, which makes physical sense as 100% reptation cannot be surpassed, and in dilute polymer solutions with no interchain entanglement, 0% reptation is expected. Videomicroscopy experiments were also performed in HEC and PEO solutions and revealed qualitatively similar DNA migration dynamics. The viscosity of these solutions was significantly higher than LPA at matching concentrations. This limited the concentration range that could be analyzed due to the constraints of our videomicroscopy setup. While experiments had to be restricted to lower C/C^* values, especially for PEO, the transition from TEC to reptation appears to be analogous to what was observed in LPA solutions.

The transition from TEC to reptation emerges at a point where polymer solution viscosity begins to increase and occurs in a regime that exhibits both semientangled and semidilute polymer solution characteristics. The transition occurs far beyond C^* and indicates that few polymer−polymer entanglements exist per chain near the overlap concentration, C^*. Moreover, the lifetimes of any existing entanglements are much shorter than required to appreciably induce the DNA molecule to enter inside a pseudopore structure within the network. Instead, when migrating DNA collides with a polymer molecule, or succession of polymer molecules, the polymer chain or chains become entangled with the DNA. This situation gives rise to the familiar transient entanglement coupling mechanism of electrophoretic DNA separation.[16,17] At a high polymer concentration, e.g., a 2% w/w LPA solution with a molecular mass of 3.5 million g/mol, a network of highly entangled polymer chains clearly exists, as evidenced by rheology. The chance for a DNA molecule to disrupt, or "unknot", polymer entanglements and drag polymers along while continuously breaking new network entanglements throughout the solution is highly improbable. Conversely in the extreme case of a 2% w/w solution of a much smaller polymer molecule (e.g., a 10 000 g/mol polymer), the polymer molecules in solution would not form a strong entangled network, and transient entanglement coupling would be the expected separation mechanism. Therefore, the probability of an electrophoretic DNA separation mechanism occurring should be thought of in terms of the degree of polymer

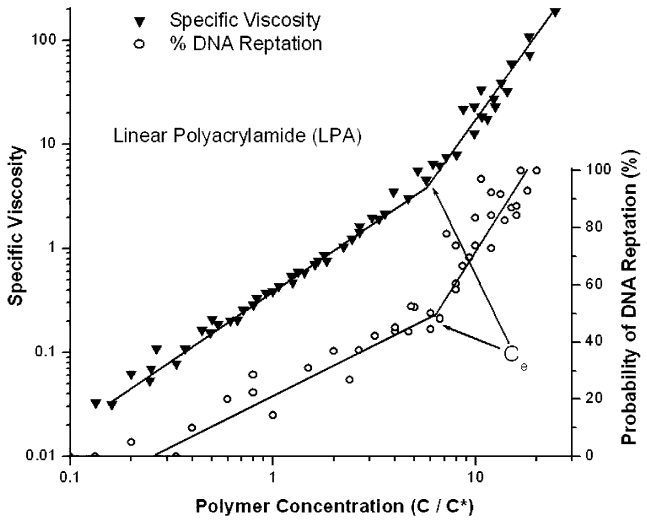

Figure 5. Specific viscosity and the probability of DNA reptation during electrophoresis each plotted against concentration relative to C^*, the overlap concentration, for three LPA polymers with molar masses of 600 000, 1 200 000, and 3 500 000 g/mol. The specific viscosity of these polymer solutions reduce down and overlap to a single trend of increasing viscosity with a marked increase in slope at the entanglement concentration, C_e, near $6.5C^*$. The probability of DNA reptation also reduces to a universal scaling with increasing probability of reptation vs polymer concentration. As with the case in the viscosity data, a marked increase in slope in reptation events develops at C_e. Lines have been drawn to guide the eye.

network entanglement, since the mechanism is a function of both polymer concentration and polymer molar mass.

Consequently, we sought to generalize our observations, by condensing all of the single-molecule videomicrosocpy data onto a universal plot. This methodology has been previously applied to create a universal scaling relationship between polymer solution viscosity and polymer concentration based on the entanglement concentration, C_e.[10] Here we wished to simultaneously examine results obtained with different molar mass polymers within the same family of polymers and have plotted the probability of the DNA separation mechanism versus the normalized concentration (C/C^*). The results of this analysis as applied to both rheological data and the probability of specific DNA separation modalities for polyacrylamide solutions are presented in Figure 5 (data for HEC and PEO shown in Supporting Information). In this figure, data for all three molar masses of polyacrylamide have been plotted versus this normalized concentration in a range from 0.1 to 11 times the overlap concentration. The specific viscosity among these polymer solutions overlaps well with little scatter and follows a power law relationship until $\sim 6.5C^*$. At this point, the slope of the viscosity data increases significantly and fits a new power law relationship. This marked increase in solution viscosity directly correlates with the polymer entanglement concentration, C_e. The imaging data also condense onto a universal curve, with somewhat more scatter than was observed for the data collected from very well-developed rheology techniques. DNA reptation events occur with low frequency at concentrations near or below $2C^*$, and the trend of increasing DNA reptation versus polymer concentration is observed. At a concentration of $\sim 6.5C^*$, the rate of increase in DNA reptation becomes notably greater. At $6.5C^*$, the probability of reptation is at 50% and quickly increases to 100%. This increase in reptation corresponds remarkably well with transitions in the rheology data, suggesting that the conversion in electrophoretic migration mechanism from transient entanglement coupling to reptation is directly related to the polymer entanglement concentration, C_e. This is the concentration at which the network becomes "elastically effective", which has clear implications for DNA migration and entanglement dynamics. This transition point has been marked on the plot in Figure 5.

Previous literature has indicated that the relationship between C_e and C^* is directly related to the number of "blobs" (or chain segments) per entanglement, n_e, as seen in eq 1.[38] For the polymer

$$C_e = n_e^{0.76} C^* \tag{1}$$

solutions we have studied, LPA, PEO, and HEC, the ratios of C_e to C^* were 6.5, 5, and 3.5, respectively. Homopolymers of differing chemical composition will have different C_e to C^* ratios due to intrinsic differences in polymers such as steric hindrances, the degree of polymer chain solvation, and intrapolymer self-interactions. This indicates that on average 11.7 blobs are involved per entanglement in LPA, 8.5 blobs per entanglement in PEO, and 4.3 in HEC. Additionally, in eq 2, we can estimate the average number of blobs per chain, N/g,[38] as a function of this same reduced concentration. By dividing the number of blobs per chain

$$N/g = (C/C^*)^{1.31} \tag{2}$$

by the number of blobs per entanglement (N/G by n_e) the number of entanglements per chain is obtained for that polymer as seen in eq 3. The outcome of this analysis indicates that for LPA (with

$$\frac{N}{g n_e} = \left(\frac{C}{C^*}\right)^{1.31} \frac{1}{n_e} \tag{3}$$

$n_e = 11.7$) at C^*, approximately 1 in 12 chains is entangled, while 1 entanglement per chain is observed at C_e, 2 entanglements per chain exist at $\sim 11C^*$, and three entanglements at $\sim 15C^*$. Re-examining Figure 5, at C^*, ~20% DNA reptation was observed, at C_e we observe 50% DNA reptation, and at $\sim 15C^*$ full reptation is observed. These reptation values parallel well with the aforementioned entanglement states. Hence, full reptation occurs in polymer solutions with an average of three entanglements per chain.

The electrophoretic mobility of λ-DNA was examined in linear polyacrylamide solutions, as shown in Figure 6, for a polymer with a weight-average molar mass of 1 200 000 g/mol. In dilute polymer solutions, the mobility of the λ-DNA remains relatively unchanged until concentrations of ~0.2% w/w are reached. As polymer concentration is further increased, the electrophoretic mobility decreases steadily with a log−log slope of −0.48, which represents a mixture of DNA migration modalities (TEC and reptation), as reptation is considerably slower than migration by TEC.[21] Also coplotted is the probability of observed DNA reptation. The concentration-dependent electrophoretic mobility mirrors the frequency of DNA reptation events observed or, alternatively, follows the decrease of TEC observed. The mobility data for λ-DNA can be roughly fit (due to the scatter present in the mechanism observation data) to the observed DNA reptation data

(38) Raspaud, E.; Lairez, D.; Adam, M. *Macromolecules* **1995**, *28*, 927−933.

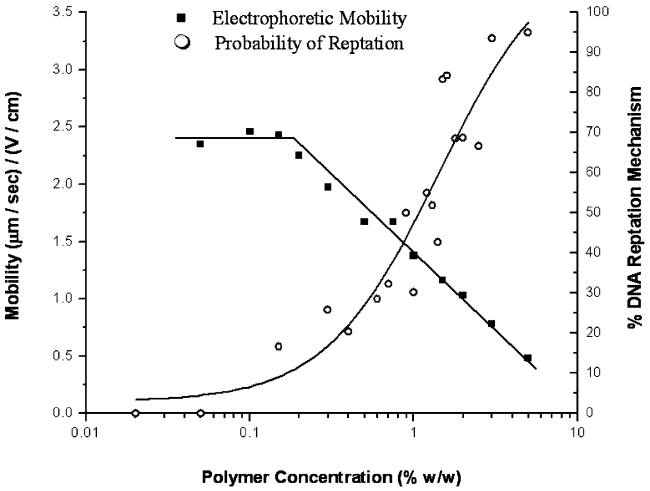

Figure 6. Polymer concentration-dependent electrophoretic mobility of λ-DNA compared to the percentage of observed reptation mechanism in LPA solutions with a molecular mass of 1.2 million g/mol. A sigmoidal fit has been applied to the reptation data, and lines have been drawn to aid the eye for DNA mobility. The mobility has a log−log slope of −0.48 at a field strength similar to imaging conditions, 94 V/cm.

using a two-parameter model for mobilities of a reptating DNA and a TEC DNA. The decrease in mobility for λ-DNA seen in increasingly entangled polymer networks is due to the decrease in faster TEC events (globular intermediates migrate more quickly) and an increase in the percentage of slower, reptating DNA.

CONCLUSIONS

The further study of DNA migration mechanisms in polymer solutions utilized in capillary and microchip electrophoresis will lead to microdevices that maximize DNA separation performance while minimizing the time required for a given separation. Understanding the underlying processes is critical to assays that rely on high-resolution, size-based DNA separations. In this work, we have shown that while C^* is a significant parameter in determining the onset of DNA reptation, the polymer entanglement concentration, C_e, is also an essential factor for assessing the degree of polymer entanglement and predicting when DNA will make the transition to a fully reptating state. The transition from TEC to reptation is moderately sharp, and we observed polymer solution concentration regimes that have both mechanisms operating simultaneously. The observed combination of mechanisms correlates qualitatively with intermediate electrophoretic mobilities. Additionally, experimental observations of TEC at higher frequencies in larger molar mass polymers are in good agreement with a longer mean polymer−DNA entanglement time.

ACKNOWLEDGMENT

The authors gratefully acknowledge Professor Wesley Burghardt for his insights into polymer solution dynamics. Financial support was provided by the Air Force Office of Scientific Research (AFOSR), the Defense Advanced Research Projects Agency (DARPA DURINT Grant F46920-01-1-0401), the NSF through the Northwestern University Nanoscale Science and Engineering Center (Award EEC-0118025), and the NIH (Grants 5 R01 HG-01970-02S1 and AI-03-017). B.E.R. was supported while on appointment as a U.S. Department of Homeland Security (DHS) Fellow under the DHS Scholarship and Fellowship Program, a program administered by the Oak Ridge Institute for Science and Education (ORISE) for DHS through an interagency agreement with the U.S Department of Energy (DOE). ORISE is managed by Oak Ridge Associated Universities under DOE contract DE-AC05-06OR23100. All opinions expressed in this paper are the authors and do not necessarily reflect the policies and views of DHS, DOE, or ORISE.

SUPPORTING INFORMATION AVAILABLE

Additional information as noted in text. This material is available free of charge via the Internet at http://pubs.acs.org.

Received for review June 1, 2007. Accepted July 26, 2007.

AC071160X